ELECTRONIC PROPERTIES
OF SOLID

Attractive Hubbard Model: Homogeneous Ginzburg–Landau Expansion and Disorder[1]

E. Z. Kuchinskii[a], N. A. Kuleeva[a], and M. V. Sadovskii[a, b]

[a] *Institute for Electrophysics, Ural Branch, Russian Academy of Sciences, Yekaterinburg, 620016 Russia*
[b] *Mikheev Institute for Metal Physics, Ural Branch, Russian Academy of Sciences, Yekaterinburg, 620290 Russia*
e-mail: kuchinsk@iep.uran.ru; sadovski@iep.uran.ru

Abstract—We derive a Ginzburg–Landau (GL) expansion in the disordered attractive Hubbard model within the combined Nozieres–Schmitt-Rink and DMFT+Σ approximation. Restricting ourselves to the homogeneous expansion, we analyze the disorder dependence of GL expansion coefficients for a wide range of attractive potentials U, from the weak BCS coupling region to the strong-coupling limit, where superconductivity is described by Bose–Einstein condensation (BEC) of preformed Cooper pairs. We show that for the a semi-elliptic "bare" density of states of the conduction band, the disorder influence on the GL coefficients A and B before quadratic and quartic terms of the order parameter, as well as on the specific heat discontinuity at the superconducting transition, is of a universal nature at any strength of the attractive interaction and is related only to the general widening of the conduction band by disorder. In general, disorder growth increases the values of the coefficients A and B, leading either to a suppression of the specific heat discontinuity (in the weak-coupling limit), or to its significant growth (in the strong-coupling region). However, this behavior actually confirms the validity of the generalized Anderson theorem, because the disorder dependence of the superconducting transition temperature T_c, is also controlled only by disorder widening of the conduction band (density of states).

1. INTRODUCTION

The problem of superconductivity in the BCS–BEC crossover region (and up to the strong coupling limit) has a long history, starting with early works by Leggett and Nozieres and Schmitt-Rink [1, 2]. Probably the simplest model to study this crossover is the Hubbard model with attractive interaction. The most successive approach to the studies of the Hubbard model (both repulsive and attractive) is the dynamical mean field theory (DMFT) [3–5]. The attractive Hubbard model was already studied within DMFT in a number of papers [6–10]. However, up to now there are only a few works where disorder effects were taken into account, either in normal or in superconducting phase of this model. Qualitative analysis of disorder effects on the critical temperature T_c in the BCS–BEC crossover region was presented in [11], which claimed the validity of the Anderson theorem in this region in the case of s-wave pairing. A diagram analysis of disorder effects on T_c and the properties of the normal state in the crossover region were recently presented in [12].

We have developed the generalized DMFT+Σ approach to the Hubbard model [13–16], which is quite convenient for including various "external"

interactions, such as disorder scattering [17, 18]. This approach is also well suited to the studies of two-particle properties, such as dynamic (optical) conductivity [17, 19]. In recent paper [10], we used this approach to analyze the single-particle properties of the normal phase and optical conductivity in the attractive Hubbard model. Subsequently, the DMFT+Σ approximation was combined with the Nozieres–Schmitt-Rink approach to study the influence of disorder on the superconducting critical temperature T_c in the BCS-BEC crossover and strong-coupling regions [20, 21], demonstrating the validity of the generalized Anderson theorem. Disorder effects on T_c are essentially due to only the general widening of the conduction band by random scattering. This was demonstrated exactly (for the whole range of attractive interactions) in the case of a semi-elliptic density of states of the conduction band (three-dimensional case) at any disorder level and is also valid in the case of a flat band (two-dimensional case) in the limit of strong enough disorder.

The Ginzburg–Landau (GL) expansion in the BCS–BEC crossover region was derived in a number of papers [22–24], but no effects of disorder scattering on the GL expansion coefficients were considered. Here, we derive the microscopic coefficients of a

[1] The article is published in the original.

(homogeneous) GL expansion for the attractive Hubbard model and study disorder effects on these coefficients including the BCS–BEC and strong-coupling regions, as well as on the specific heat discontinuity at the superconducting transition, demonstrating a certain universality of disorder behavior of these characteristics.

2. DISORDERED HUBBARD MODEL IN THE DMFT+Σ APPROACH

We consider the disordered attractive Hubbard model with the Hamiltonian

$$H = -t \sum_{\langle ij \rangle \sigma} a_{i\sigma}^\dagger a_{j\sigma} + \sum_{i\sigma} \epsilon_i n_{i\sigma} - U \sum_i n_{i\uparrow} n_{i\downarrow}, \quad (1)$$

where $t > 0$ is a transfer integral between the nearest neighbors and U is the onsite Hubbard attraction, $n_{i\sigma} = a_{i\sigma}^\dagger a_{i\sigma}$ is electron number operator at site i, and $a_{i\sigma}$ ($a_{i\sigma}^\dagger$) is the annihilation (creation) operator of an electron with spin σ. Local energy levels ϵ_i are assumed to be independent random variables on different lattice sites. We assume the Gaussian distribution of ϵ_i at each site for the validity of the standard "impurity" scattering diagram technique [25]:

$$\mathcal{P}(\epsilon_i) = \frac{1}{\sqrt{2\pi}\Delta} \exp\left(-\frac{\epsilon_i^2}{2\Delta^2} \right). \quad (2)$$

Here, Δ is the measure of disorder scattering.

The generalized DMFT+Σ approach [13–16] supplies the standard DMFT [3–5] with an additional "external" self-energy (in general, momentum dependent) due to any interaction outside the DMFT, which provides an effective method to calculate both single- and two-particle properties [17, 19]. The additive form of the total self-energy preserves the structure of the self-consistent DMFT equations [3–5]. The "external" self-energy is recalculated at each step of the standard DMFT iteration scheme, using some approximations corresponding to the form of the additional interaction, while the local Green's function (central for DMFT) is also "dressed" by the additional interaction.

For the disordered Hubbard model, we take the "external" self-energy entering the DMFT+Σ loop in the simplest form of a self-consistent Born approximation, neglecting the "crossing" diagrams due to disorder scattering:

$$\tilde{\Sigma}(\epsilon) = \Delta^2 \sum_{\mathbf{p}} G(\epsilon, \mathbf{p}), \quad (3)$$

where $G(\epsilon, \mathbf{p})$ is the complete single-particle Green's function.

To solve the effective Anderson impurity model of DMFT, we here use the effective algorithm of the numerical renormalization group (NRG) [26].

In what follows, we consider the model of a "bare" conduction band with the semi-elliptic density of states (per unit cell and spin projection)

$$N_0(\epsilon) = \frac{2}{\pi D^2} \sqrt{D^2 - \epsilon^2}, \quad (4)$$

where D determines the half-width of the conduction band. This is a good approximation in the three-dimensional case.

In [21], we have shown analytically that in the DMFT+Σ approach, within these approximations, all the disorder influence on the single-particle properties reduces to the simple effect of band widening by disorder scattering, $D \to D_{\text{eff}}$, where D_{eff} is the effective band half-width in the presence of disorder (in the absence of correlations, i.e., for $U = 0$):

$$D_{\text{eff}} = D \sqrt{1 + 4 \frac{\Delta^2}{D^2}}, \quad (5)$$

and the conduction band density of states (in the absence of U) "dressed" by disorder is given by

$$\tilde{N}_0(\epsilon) = \frac{2}{\pi D_{\text{eff}}^2} \sqrt{D_{\text{eff}}^2 - \epsilon^2}, \quad (6)$$

preserving its semi-elliptic form.

For other models of the "bare" conduction band density of states, besides band widening, disorder scattering changes the form of the density of states, and hence the complete universality of disorder influence of single-particle properties, strictly speaking, is absent. But in the limit of strong enough disorder, the "bare" band density effectively becomes elliptic for any reasonable model, and the universality is thus restored [21].

All calculation below were performed for the quarter-filled band ($n = 0.5$ per lattice site).

3. GINZBURG–LANDAU EXPANSION

The critical temperature of the superconducting transition T_c in the attractive Hubbard model was analyzed using direct DMFT calculations in a number of papers [6, 7, 9]. In [10], we determined T_c from the instability condition of the normal phase (instability of the DMFT iteration procedure). The results obtained in this way were in good agreement with the results in [6, 7, 9]. Additionally, in [10], we calculated T_c using the approximate Nozieres–Schmitt-Rink approach in combination with DMFT (used to calculate the chemical potential of the system), demonstrating that being much less time consuming, it provides a semi-quantitative description of the T_c behavior in the BCS–BEC crossover region, in good agreement with direct DMFT calculations. In [20, 21], the combined Nozieres–Schmitt-Rink approach was used to study the detailed dependence of T_c on disorder. Below, we use this combined approach to derive the GL expan-
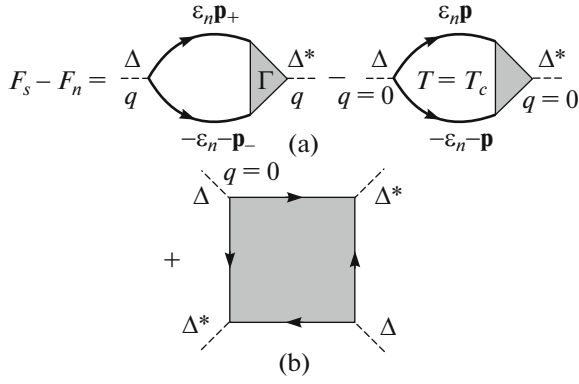
Fig. 1. Diagram representation of the Ginzburg–Landau expansion.

sion including the disorder dependence of the GL expansion coefficients.

We write the GL expansion for the difference of free energies of superconducting and normal phases in the standard form

$$F_s - F_n = A|\Delta_{\mathbf{q}}|^2 + q^2 C|\Delta_{\mathbf{q}}|^2 + \frac{B}{2}|\Delta_{\mathbf{q}}|^4, \quad (7)$$

where $\Delta_{\mathbf{q}}$ is the spatial Fourier component of the amplitude of the superconducting order parameter. Microscopically, this expansion is determined by diagrams of the loop expansion for the free energy of an electron in the "external field" of (static) superconducting order parameter fluctuations with a small wave vector $\mathbf{q}$, shown in Fig. 1 (where fluctuations are represented by dashed lines) [25]. Below, we limit ourselves to the case of a homogeneous expansion with $\mathbf{q} = 0$ and calculations of its coefficients A and B, leaving the (much more complicated) analysis of the general inhomogeneous case of finite $\mathbf{q}$ and calculations of the coefficient C in (7) for the future work.

Within the Nozieres–Schmitt-Rink approach [2], we use the weak-coupling approximation to calculate loop diagrams with two and four Cooper vertices shown in Fig. 1, dropping all corrections due to the Hubbard U, while including "dressing" by disorder scattering.[2] However, the chemical potential, which essentially depends on the coupling strength U and determines the BEC condition in the strong-coupling region, is calculated via the full DMFT+Σ procedure.

The coefficient A before the square of the order parameter in the GL expansion is given by the diagrams in Fig. 1a with $q = 0$ [25]:

$$A(T) = \chi_0(q = 0, T) - \chi_0(q = 0, T_c), \quad (8)$$

where

---

[2]In the absence of disorder, this approach just coincides with that used in [22–24], involving the Hubbard–Stratonovich transformation in the functional integral over fluctuations of the superconducting order parameter.

$$\chi_0(q = 0, T) = -T\sum_n \sum_{\mathbf{pp'}} \Phi_{\mathbf{pp'}}(\varepsilon_n) \quad (9)$$

is the two-particle loop in the Cooper channel "dressed" only by disorder scattering, while $\Phi_{\mathbf{pp'}}(\varepsilon_n)$ is the disorder-averaged two-particle Green's function in the Cooper channel ($\varepsilon_n = \pi T(2n + 1)$ is the corresponding Matsubara frequency). Subtraction of the second diagram in Fig. 1a, i.e., that of $\chi_0(q = 0, T_c)$ in (8), guarantees the validity of $A(T = T_c) = 0$, which necessarily holds in any kind of Landau expansion [25].

To obtain $\sum_{\mathbf{pp'}} \Phi_{\mathbf{pp'}}(\varepsilon_n)$, we use the exact Ward identity derived in [19]:

$$G(\varepsilon_n, \mathbf{p}) - G(-\varepsilon_n, -\mathbf{p}) = -\sum_{\mathbf{p'}} \Phi_{\mathbf{pp'}}(\varepsilon_n)$$
$$\times (G_0^{-1}(\varepsilon_n, \mathbf{p'}) - G_0^{-1}(-\varepsilon_n, -\mathbf{p'})). \quad (10)$$

Here, $G(\varepsilon_n, \mathbf{p})$ is the disorder-averaged single-particle Green's function (not "dressed" by Hubbard interaction!). With the symmetry $\varepsilon(\mathbf{p}) = \varepsilon(-\mathbf{p})$ and $G(\varepsilon_n, -\mathbf{p}) = G(\varepsilon_n, \mathbf{p})$, we use Ward identity (10) to obtain

$$\sum_{\mathbf{pp'}} \Phi_{\mathbf{pp'}}(\varepsilon_n) = -\frac{\sum_{\mathbf{p}} G(\varepsilon_n, \mathbf{p}) - \sum_{\mathbf{p}} G(-\varepsilon_n, \mathbf{p})}{2i\varepsilon_n}, \quad (11)$$

whence we obtain Cooper susceptibility (9)

$$\chi_0(q = 0, T) = T\sum_n \frac{\sum_{\mathbf{p}} G(\varepsilon_n, \mathbf{p}) - \sum_{\mathbf{p}} G(-\varepsilon_n, \mathbf{p})}{2i\varepsilon_n}$$
$$= T\sum_n \frac{\sum_{\mathbf{p}} G(\varepsilon_n, \mathbf{p})}{i\varepsilon_n}. \quad (12)$$

Performing the standard summation over Matsubara frequencies [25], we now obtain

$$\chi_0(q = 0, T)$$
$$= \frac{1}{4\pi i}\int_{-\infty}^{\infty} d\varepsilon \frac{\sum_{\mathbf{p}} G^R(\varepsilon, \mathbf{p}) - \sum_{\mathbf{p}} G^A(\varepsilon, \mathbf{p})}{\varepsilon} \tanh\frac{\varepsilon}{2T} \quad (13)$$
$$= -\int_{-\infty}^{\infty} d\varepsilon \frac{\tilde{N}(\varepsilon)}{2\varepsilon} \tanh\frac{\varepsilon}{2T},$$

where $\tilde{N}(\varepsilon)$ is the "bare" ($U = 0$) density of states "dressed" by disorder scattering, which in the case of a semi-elliptic band takes the form (6). In Eq. (13), the origin of ε is at the chemical potential. Replacing $\varepsilon \rightarrow \varepsilon - \mu$ to shift the origin of energy to the center of conduction band, we finally write

$$\chi_0(q = 0, T) = -\int_{-\infty}^{\infty} d\varepsilon \frac{\tilde{N}(\varepsilon)}{2(\varepsilon - \mu)} \tanh \frac{\varepsilon - \mu}{2T}. \quad (14)$$

The Cooper instability of the normal phase, determining the superconducting transition temperature T_c, is written as

$$1 = -U\chi_0(q = 0, T_c). \quad (15)$$

We then obtain the following equation for the critical temperature:

$$1 = \frac{U}{2} \int_{-\infty}^{\infty} d\varepsilon \tilde{N}_0(\varepsilon) \frac{\tanh((\varepsilon - \mu)/2T_c)}{\varepsilon - \mu}. \quad (16)$$

Using (15) to determine $\chi_0(q = 0, T_c)$ and (14) for $\chi_0(q = 0, T)$, we obtain the coefficient A in (8):

$$A(T) = \frac{1}{U} - \int_{-\infty}^{\infty} d\varepsilon \tilde{N}_0(\varepsilon) \frac{\tanh((\varepsilon - \mu)/2T)}{2(\varepsilon - \mu)}. \quad (17)$$

The chemical potential for different values of U and Δ is to be determined here from direct DMFT+Σ calculations, i.e., from the standard equation for the total number of electrons (band filling), defined by the Green's function obtained in the DMFT+Σ approximation. This allows us to find both T_c and GL expansion coefficients in a wide range of parameters of the model, including the BCS−BEC crossover region and the limit of strong coupling, for different disorder levels. Actually, this is the essence of the Nozieres−Schmitt-Rink approximation in the weak-coupling region, transition temperature is controlled by the equation for Cooper instability, while in the strong-coupling limit, it is defined as the temperature of Bose condensation, which is controlled by the equation for the chemical potential. The joint solution of Eqs. (16) and (17) with the DMFT+Σ equation for the chemical potential provides the correct interpolation for T_c and GL coefficient A from the weak-coupling region via the BCS−BEC crossover towards the strong coupling.

For $T \to T_c$, the coefficient $A(T)$ is written as

$$A(T) \equiv a(T - T_c), \quad (18)$$

where in the case of a temperature independent chemical potential,

$$a = \frac{1}{4T_c^2} \int_{-\infty}^{\infty} d\varepsilon \tilde{N}_0(\varepsilon) \frac{1}{\cosh^2((\varepsilon - \mu)/2T_c)}. \quad (19)$$

In the BCS approximation with the conduction band of an infinite width with a constant density of states $\tilde{N}_0(0)$, we obtain the standard result $a = \tilde{N}_0(0)/T_c$ from (19) [25]. However, in the BCS−BEC crossover region, the temperature dependence of μ is essential and we have to use the general expression (17) in conjunction with the equation for μ to calculate a. At the same time, it is clear from Eq. (17) that disorder

scattering influences a only through the changes of the density of states $\tilde{N}_0(\varepsilon)$ and the chemical potential μ, which is a typical single-particle property. Thus, in the case of a semi-elliptic "bare" conduction band, the dependence of a on disorder is due to only the band widening by disorder, with the replacement $D \to D_{\text{eff}}$. Therefore, in the presence of disorder, we expect the universal dependence of $a(2D_{\text{eff}})^2$ on $U/2D_{\text{eff}}$ (all energies are to be normalized by the effective bandwidth $2D_{\text{eff}}$), which is confirmed by the results of direct numerical computations in the next section (cf. Fig. 4a).

The coefficient B is determined by a "square" diagram with four Cooper vertices with $q = 0$, "dressed" in an arbitrary way by disorder scattering, which is shown in Fig. 1b [25]:

$$B = \frac{1}{2} T \sum_n \sum_{\mathbf{p}_1 \mathbf{p}_2 \mathbf{p}_3 \mathbf{p}_4} \langle G(i\varepsilon_n; \mathbf{p}_1, \mathbf{p}_2) G(-i\varepsilon_n; -\mathbf{p}_2, -\mathbf{p}_3) \\ \times G(i\varepsilon_n; \mathbf{p}_3, \mathbf{p}_4) G(-i\varepsilon_n; -\mathbf{p}_4, -\mathbf{p}_1) \rangle, \quad (20)$$

where $\langle ... \rangle$ denotes averaging over disorder, and $G(i\varepsilon_n; \mathbf{p}_1, \mathbf{p}_2)$ (and other similar expressions) represent exact single-particle Green's functions for a fixed configuration of the random potential. Performing standard summation over Matsubara frequencies, we obtain

$$B = \frac{1}{2} \int_{-\infty}^{\infty} \frac{d\varepsilon}{2\pi i} \tanh \frac{\varepsilon}{2T} \\ \times \sum_{\mathbf{p}_1 \mathbf{p}_2 \mathbf{p}_3 \mathbf{p}_4} \langle G^R(\varepsilon; \mathbf{p}_1, \mathbf{p}_2) G^A(\varepsilon; -\mathbf{p}_2, -\mathbf{p}_3) \quad (21) \\ \times G^R(\varepsilon; \mathbf{p}_3, \mathbf{p}_4) G^A(-\varepsilon; -\mathbf{p}_4, -\mathbf{p}_1) \rangle.$$

Due to the zero momentum $\mathbf{q} = 0$ in Cooper vertices and the static nature of disorder scattering, we can now use a certain generalization of Ward identity (10) to obtain (at $T = T_c$)

$$B = \int_{-\infty}^{\infty} \frac{d\varepsilon}{4\varepsilon^3} \left(\tanh \frac{\varepsilon}{2T_c} - \frac{\varepsilon/2T_c}{\cosh^2 \varepsilon/2T_c} \right) \tilde{N}_0(\varepsilon). \quad (22)$$

A detailed derivation is presented in Appendix A. In the BCS approximation, using the conduction band of an infinite width with a constant density of states $\tilde{N}_0(0)$, we immediately obtain the standard result from Eq. (22): $B = (7\zeta(3)/8\pi^2 T_c^2) \tilde{N}_0(0)$ [25].

Again, replacing here $\varepsilon \to \varepsilon - \mu$ to shift the origin of energy to the middle of the conduction band, we can write
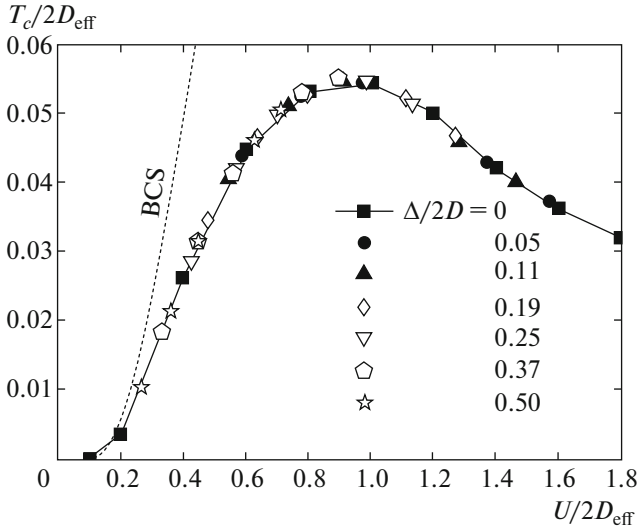
Fig. 2. Universal dependence of the superconducting critical temperature on disorder for different values of the Hubbard attraction.

$$B = \int_{-\infty}^{\infty} \frac{d\varepsilon}{4(\varepsilon - \mu)^3}$$

$$\times \left(\tanh\frac{\varepsilon - \mu}{2T_c} - \frac{(\varepsilon - \mu)/2T_c}{\cosh^2\frac{\varepsilon - \mu}{2T_c}} \right) \tilde{N}_0(\varepsilon). \tag{23}$$

It follows that the disorder dependence of the coefficient B (similarly to A) is also determined only by the disorder-widened density of states $\tilde{N}_0(\varepsilon)$ and the chemical potential, and hence in the case of a semi-

elliptic "bare" conduction band, it reduces to the simple replacement $D \rightarrow D_{\text{eff}}$, leading to a universal dependence of $B(2D_{\text{eff}})^3$ on $U/2D_{\text{eff}}$, which is confirmed by the results of direct numerical computations presented in the next section and shown in Fig. 4b.

We stress that Eqs. (17) and (23) for the GL coefficients A and B were obtained with the use of exact Ward identities, and are therefore valid also in the limit of strong disorder (beyond Anderson localization).

The universal dependence on disorder, related to the conduction band widening by disorder scattering, is also valid for the specific-heat discontinuity at T_c, because it is completely determined by the coefficients a and B:

$$C_s(T_c) - C_n(T_c) = T_c \frac{a^2}{B}. \tag{24}$$

Appropriate numerical results are also given in the next Section (cf. Fig. 5b).

The coefficient C before the gradient term of the GL expansion is determined essentially by two-particle characteristics (in particular, due to a nontrivial q-dependence of the vertex, which is obviously changed by disorder scattering). In particular, the behavior of C is significantly changed at the Anderson transition [27], and therefore no universality of the disorder dependence is expected in this case.

4. MAIN RESULTS

We now discuss the main results of our numerical calculations, directly demonstrating the universal dependences of the GL coefficients A and B and the specific heat discontinuity at T_c on disorder.

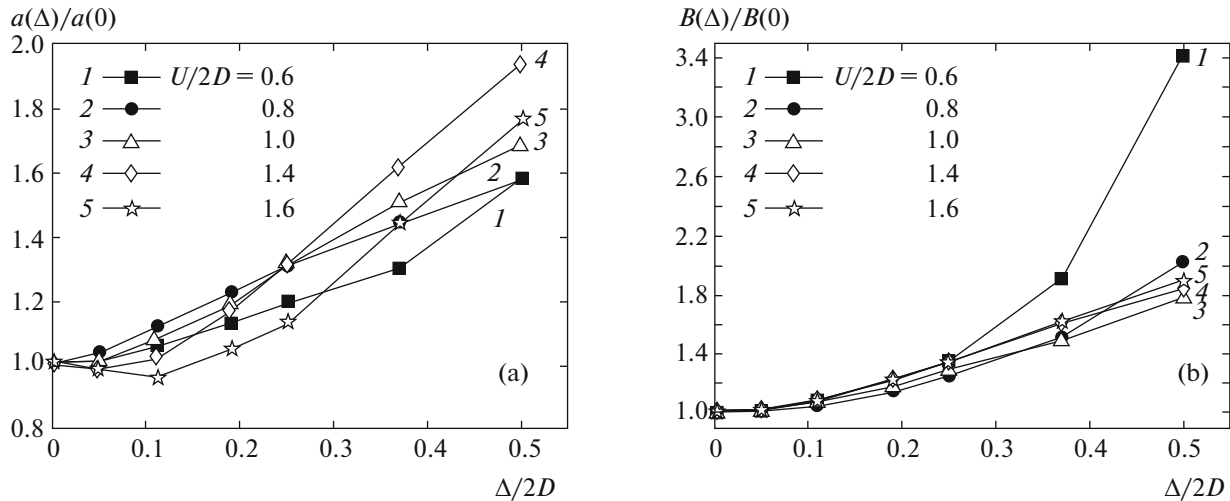In Fig. 2, we show the universal dependence of the critical temperature T_c on the Hubbard attraction U for

Fig. 3. Disorder dependence of the GL coefficients (a) a and (b) B, normalized by their values in the absence of disorder, for different values of the Hubbard attraction.
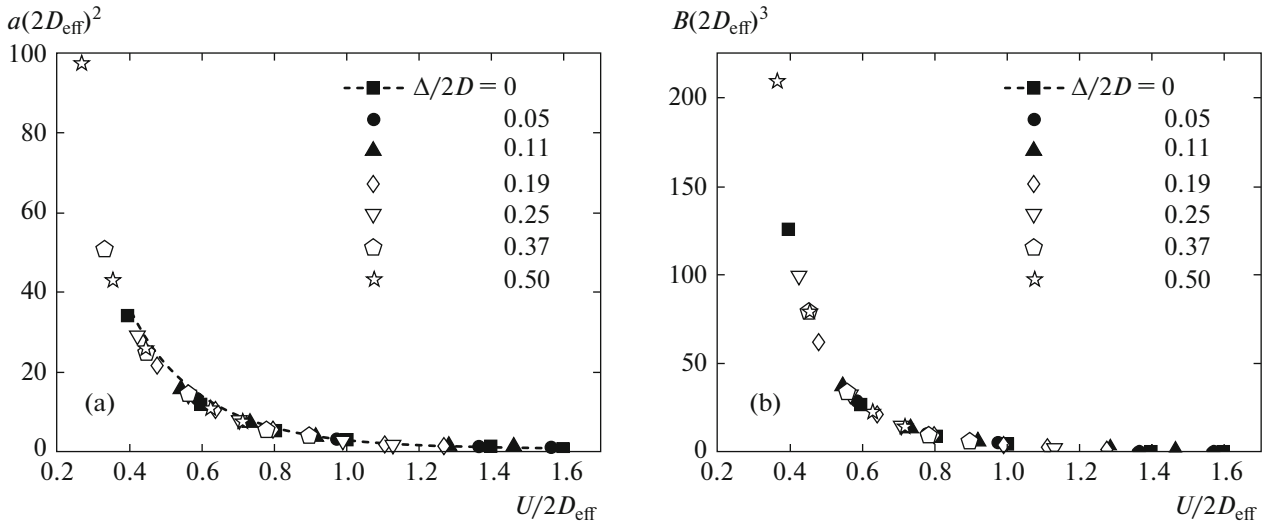
Fig. 4. Universal dependence of the GL coefficients (a) a and (b) B on the Hubbard attraction for different values of disorder.
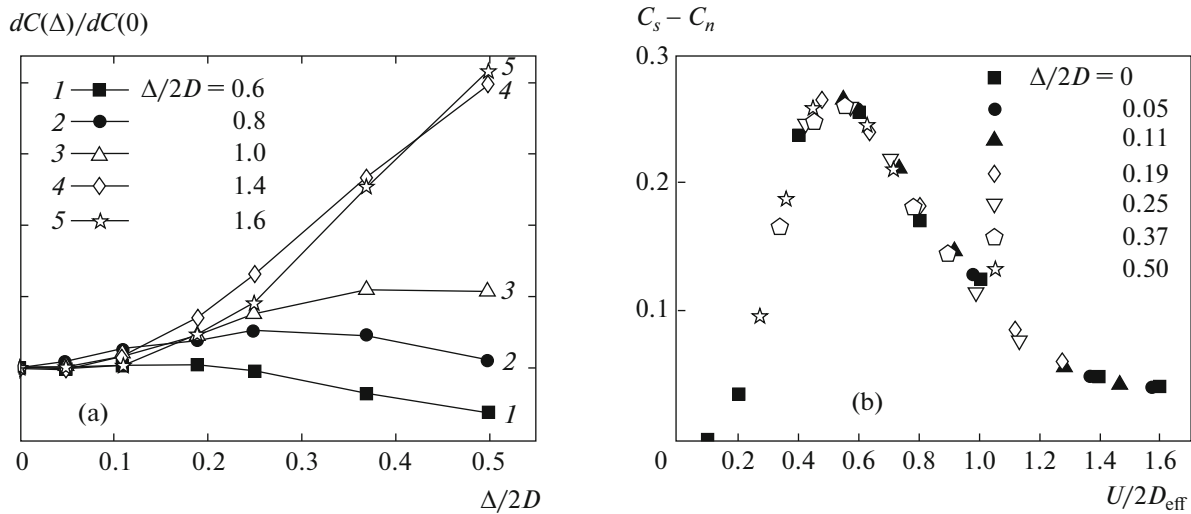

Fig. 5. (a) Dependence of the specific heat discontinuity at the critical temperature, $dC \equiv C_s - C_n$, on disorder for different values of the Hubbard attraction U and (b) universal dependence of this discontinuity on U for different values of disorder.

different levels of disorder, which was obtained and discussed in detail in [20, 21]. A typical maximum of T_c at $U/2D_{eff} \sim 1$ is characteristic of the BCS–BEC crossover region.

In Fig. 3, we present disorder dependences of the GL coefficients a (Fig. 3a) and B (Fig. 3b) for different values of the Hubbard attraction. We can see that a in general increases with an increase in disorder. Only in the limit of a strong enough coupling $U/2D > 1.4$ (curves 4 and 5) in the region of weak disorder do we observe weak suppression of a by disorder scattering. The coefficient B grows sufficiently fast with disorder in the region of weak coupling (curve 1 in Fig. 3b),

while in the region of strong coupling, this growth becomes more moderate (curves 4, 5 in Fig. 3b), such that the dependence of B on disorder in this region becomes almost independent of the value of U (curves 4 and 5 practically coincide).

However, this rather complicated dependence of the coefficients a and B on disorder is determined solely by the growth of the effective conduction bandwidth with disorder, given by Eq. (5). In Fig. 4, we show the universal dependences of the GL coefficients a and B, normalized by appropriate powers of the effective bandwidth, on the strength of Hubbard attraction. In the absence of disorder (the dashed line
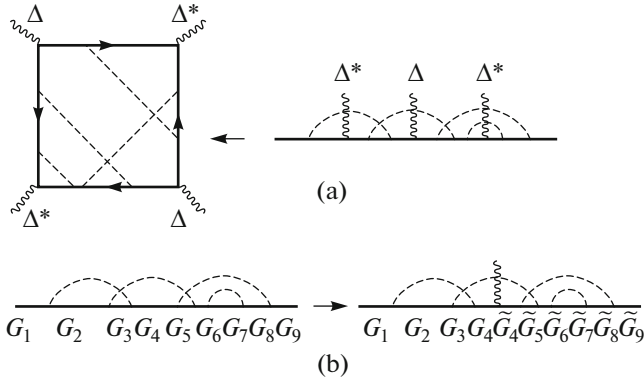
Fig. 6. Diagrams for the coefficient B and the derivation of a generalized Ward identity.

with squares), the coefficients a and B decrease fast as U increases. Other symbols in Fig. 4 show the results of our calculations for different levels of disorder. It is clearly seen that all the data ideally fit the universal curve obtained in the absence of disorder.

The coefficients a and B determine the specific heat discontinuity at the critical temperature, Eq. (24). Because these coefficients and T_c [20, 21] depend on disorder in a universal way due only to the growth of the effective bandwidth (5), the same type of universal dependence is also valid for the specific heat discontinuity. In Fig. 5a, we show the dependence of the specific heat discontinuity $dC \equiv C_s - C_n$ on disorder for different values of the Hubbard attraction U. It is seen that in the region of weak coupling (curve *1*), the specific heat discontinuity is suppressed by disorder; for intermediate couplings (curves *2* and *3*), weak disorder leads to an increase in the specific heat discontinuity, while further increasing the disorder suppresses this discontinuity. In the region of strong coupling (curves *4* and *5*), the increase in disorder leads to a significant increase in the specific heat discontinuity, which is mainly related to the similar increase in T_c (cf. [20, 21]). However, this complicated dependence of the specific heat discontinuity on disorder is again completely determined by the growth of effective bandwidth (5). In Fig. 5b, we show the universal dependence of the specific heat discontinuity on U, normalized by the bandwidth $2D_{\text{eff}}$. Black squares represent data in the absence of disorder. Other symbols in Fig. 5b show the data for different disorder levels. We see again that all the data precisely fit the universal dependence of the specific heat discontinuity obtained in the absence of disorder. The specific heat discontinuity increases with an increases in U in the region of weak coupling $U/2D_{\text{eff}} \ll 1$ and decreases with an increase in U in the limit of strong coupling $U/2D_{\text{eff}} \gg 1$. The maximum of the specific heat discontinuity is observed at $U/2D_{\text{eff}} \approx 0.55$. Actually, this dependence of the specific heat discontinuity qualita-

tively resembles a similar dependence of the critical temperature, although its maximum is attained at smaller values of the Hubbard attraction.

5. CONCLUSION

Using a combination of the Nozieres–Schmitt-Rink approximation with the generalized DMFT+Σ approach, we have studied disorder influence on the coefficients A and B determining the homogeneous Ginzburg–Landau expansion and specific heat discontinuity at the superconducting transition in the attractive Hubbard model.

We have demonstrated analytically that in the case of a "bare" conduction band with a semi-elliptic density of states, disorder influence on the GL coefficients A and B and the specific heat discontinuity is universal and is controlled only by the general conduction band (density of states) widening by disorder scattering; we illustrated this conclusion with explicit numerical calculations performed for a wide range of attractive potentials U, from the weak-coupling region, where $U/2D_{\text{eff}} \ll 1$ and the superconducting instability is described by the usual BCS approach, to the strong-coupling region, where $U/2D_{\text{eff}} \gg 1$ and the superconducting transition is determined by Bose–Einstein condensation of preformed Cooper pairs.

These results essentially prove the validity of the generalized Anderson theorem in the BCS–BEC crossover region and in the limit of strong coupling not only for T_c [20, 21] but also for the homogeneous Ginzburg–Landau expansion, determining appropriate thermodynamic effects like the specific heat discontinuity at the transition point.

APPENDIX

The Coefficient B in the Presence of Disorder

The coefficient B is determined by the "square" diagram with four Cooper vertices with $\mathbf{q} = 0$, "dressed" by disorder scattering, shown in Fig. 1b. The corresponding analytic expression is given in Eq. (20). After the standard summation over Matsubara frequencies, B is written as in (21), i.e., is determined by the following combination of four Green's functions with real frequencies:

$$\sum_{\mathbf{p}_1\mathbf{p}_2\mathbf{p}_3\mathbf{p}_4} \langle G^R(\varepsilon; \mathbf{p}_1, \mathbf{p}_2) G^A(-\varepsilon; -\mathbf{p}_2, -\mathbf{p}_3) \times G^R(\varepsilon; \mathbf{p}_3, \mathbf{p}_4) G^A(-\varepsilon; -\mathbf{p}_4, -\mathbf{p}_1) \rangle, \quad \text{(A.1)}$$

where $\langle ... \rangle$ denotes averaging over disorder and $G^{R(A)}(\varepsilon; \mathbf{p}_1, \mathbf{p}_2)$ are the exact retarded (advanced) single-particle Green's functions for a fixed configuration of disorder.

A typical diagram of the fourth order of disorder scattering (dashed lines) is shown in Fig. 6a. Arbitrary diagrams for such a four-particle Green's function can be obtained from diagrams for the single-particle Green's function of the same order of disorder scattering by arbitrarily inserting three Cooper vertices into the "bare" electron Green's functions, as shown in Fig. 6a. Taking the static nature of disorder scattering and the zero transferred momentum $\mathbf{q} = 0$ in Cooper vertices into account, we can evaluate (A.1) using a certain generalization of exact Ward identity (10), derived in [19].

We take the diagram for the single-particle Green' function, shown in the left part of Fig. 6b, and consider a certain configuration of momenta transferred by dashed lines. Here, we have nine "bare" electron Green's functions with momenta $\mathbf{p}_1, ..., \mathbf{p}_9$. In what follows, we use the short notation

$$G_i = G_0^R(\varepsilon; \mathbf{p}_i), \quad \tilde{G}_i = G_0^A(-\varepsilon; -\mathbf{p}_i), \qquad (A.2)$$

where $G_0^{R(A)}(\varepsilon; \mathbf{p}) = 1/(\varepsilon - \varepsilon(\mathbf{p}) \pm i\delta)$ is the "bare" Green's function. Inserting a Cooper vertex leads to the sign change of momenta and frequencies (i.e., to the replacement $G_i \leftrightarrow \tilde{G}_i$) in all Green's functions standing to the right of the vertex. We assume that the central of the three Cooper vertices was inserted into the fourth Green's function, as shown in the right part of Fig. 6b. An arbitrary insertion of the first Cooper vertex into one of the first four of the Green's functions leads to the result

$$G_1 G_2 C_3 G_4 \rightarrow G_1 \tilde{G}_1 \tilde{G}_2 \tilde{G}_3 \tilde{G}_4 + G_1 G_2 \tilde{G}_2 \tilde{G}_3 \tilde{G}_4 \\ + G_1 G_2 G_3 \tilde{G}_3 \tilde{G}_4 + G_1 G_2 G_3 G_4 \tilde{G}_4, \qquad (A.3)$$

whence, using the identify $G_i^{-1} - \tilde{G}_i^{-1} = 2\varepsilon$, we obtain

$$G_1 \tilde{G}_1 \tilde{G}_2 \tilde{G}_3 \tilde{G}_4 \frac{G_1^{-1} - \tilde{G}_1^{-1}}{2\varepsilon} + ... \\ + G_1 G_2 G_3 G_4 \tilde{G}_4 \frac{G_4^{-1} - \tilde{G}_4^{-1}}{2\varepsilon} = \frac{\tilde{G}_1 \tilde{G}_2 \tilde{G}_3 \tilde{G}_4 - G_1 G_2 C_3 G_4}{2\varepsilon}. \qquad (A.4)$$

Then $\tilde{G}_4 \tilde{G}_5 \tilde{G}_6 \tilde{G}_7 \tilde{G}_8 \tilde{G}_9 \rightarrow G_4 G_5 G_6 G_7 G_8 G_9$ and after all insertions of the last (third) Cooper vertex into one of the six Green's functions $G_4, ..., G_9$, we again obtain $(\tilde{G}_4 \tilde{G}_5 \tilde{G}_6 \tilde{G}_7 \tilde{G}_8 \tilde{G}_9 - G_4 G_5 G_6 G_7 G_8 G_9)/2\varepsilon$.

We thus obtain

$$\langle G^R(\varepsilon) G^A(-\varepsilon) G^R(\varepsilon) G^A(-\varepsilon) \rangle \\ = \left\langle \frac{G^A(-\varepsilon) - G^R(\varepsilon)}{2\varepsilon} \frac{G^A(-\varepsilon) - G^R(\varepsilon)}{2\varepsilon} \right\rangle \\ = \frac{1}{4\varepsilon^2} (\langle G^A(-\varepsilon) G^A(-\varepsilon) \rangle + \langle G^R(\varepsilon) G^R(\varepsilon) \rangle \qquad (A.5)$$

$$-2\langle G^R(\varepsilon) G^A(-\varepsilon) \rangle) = \frac{1}{4\varepsilon^2} \left\{ \frac{d}{d\varepsilon} (\langle G^A(-\varepsilon) \rangle - \langle G^R(\varepsilon) \rangle) \\ - \frac{\langle G^A(-\varepsilon) \rangle - \langle G^R(\varepsilon) \rangle}{\varepsilon} \right\},$$

where we can evaluate the two-particle Green's functions with $q = 0$ again using an analogue of Ward identity (10) for real frequencies. Using (A.5) in (21) and replacing $\varepsilon \rightarrow -\varepsilon$ in terms with $\langle G^A(-\varepsilon) \rangle$ in the integral over ε, we obtain

$$B = \int\limits_{-\infty}^{\infty} \frac{d\varepsilon}{2\pi i} \frac{\tanh(\varepsilon/2T)}{4\varepsilon^2} \left(\frac{d}{d\varepsilon} - \frac{1}{\varepsilon} \right) \\ \times \left(\sum_{\mathbf{p}} G^A(\varepsilon, \mathbf{p}) - \sum_{\mathbf{p}} G^R(\varepsilon, \mathbf{p}) \right) \qquad (A.6)$$

$$= \int\limits_{-\infty}^{\infty} d\varepsilon \frac{\tanh(\varepsilon/2T)}{4\varepsilon^2} \left(\frac{d}{d\varepsilon} - \frac{1}{\varepsilon} \right) \tilde{N}_0(\varepsilon)$$

$$= \int\limits_{-\infty}^{\infty} \frac{d\varepsilon}{4\varepsilon^3} \left(\tanh \frac{\varepsilon}{2T} - \frac{\varepsilon/2T}{\cosh^2(\varepsilon/2T)} \right) \tilde{N}_0(\varepsilon).$$

This expression was used in the main part of the paper.

REFERENCES

1. A. J. Leggett, in *Modern Trends in the Theory of Condensed Matter,* Ed. by A. Pekalski and J. Przystawa (Springer, Berlin, 1980).

2. P. Nozieres and S. Schmitt-Rink, J. Low Temp. Phys. **59**, 195 (1985).

3. Th. Pruschke, M. Jarrell, and J. K. Freericks, Adv. Phys. **44**, 187 (1995).

4. A. Georges, G. Kotliar, W. Krauth, and M. J. Rozenberg, Rev. Mod. Phys. **68**, 13 (1996).

5. D. Vollhardt, in *Lectures on the Physics of Strongly Correlated Systems XIV,* Ed. by A. Avella and F. Mancini, AIP Conf. Proc., Vol. 1297 (Amer. Inst. Physics, Melville, New York, 2010), p. 339; arXiv: 1004.5069.

6. M. Keller, W. Metzner, and U. Schollwock, Phys. Rev. Lett. **86**, 4612 (2001); arXiv: cond-mat/0101047.

7. A. Toschi, P. Barone, M. Capone, and C. Castellani, New J. Phys. **7**, 7 (2005); arXiv: cond-mat/0411637v1.

8. J. Bauer, A. C. Hewson, and N. Dupis, Phys. Rev. B **79**, 214518 (2009); arXiv: 0901.1760v2.

9. A. Koga and P. Werner, Phys. Rev. A **84**, 023638 (2011); arXiv: 1106.4559v1.

10. N. A. Kuleeva, E. Z. Kuchinskii, and M. V. Sadovskii, J. Exp. Theor. Phys. **119**, 264 (2014); arXiv: 1401.2295.

11. A. I. Posazhennikova and M. V. Sadovskii, JETP Lett. **65**, 270 (1997).

12. F. Palestini and G. C. Strinati, arXiv: 1311.2761.

13. E. Z. Kuchinskii, I. A. Nekrasov, and M. V. Sadovskii, JETP Lett. **82**, 198 (2005); arXiv: cond-mat/0506215.

14. M. V. Sadovskii, I. A. Nekrasov, E. Z. Kuchinskii, Th. Pruschke, and V. I. Anisimov, Phys. Rev. B **72**, 155105 (2005); arXiv: cond-mat/0508585.

15. E. Z. Kuchinskii, I. A. Nekrasov, and M. V. Sadovskii, J. Low Temp. Phys. **32**, 528 (2006); arXiv: cond-mat/0510376.

16. E. Z. Kuchinskii, I. A. Nekrasov, and M. V. Sadovskii, Phys. Usp. 55, 325 (2012); arXiv: 1109. 2305.

17. E. Z. Kuchinskii, I. A. Nekrasov, and M. V. Sadovskii, J. Exp. Theor. Phys. **106**, 581 (2008); arXiv: 0706.2618.

18. E. Z. Kuchinskii, N. A. Kuleeva, I. A. Nekrasov, and M. V. Sadovskii, J. Exp. Theor. Phys. **110**, 325 (2010); arXiv: 0908.3747.

19. E. Z. Kuchinskii, I. A. Nekrasov, and M. V. Sadovskii, Phys. Rev. B **75**, 115102 (2007); arXiv: cond-mat/0609404.

20. E. Z. Kuchinskii, N. A. Kuleeva, and M. V. Sadovskii, JETP Lett. **100**, 192 (2014); arXiv: 1406.5603.

21. E. Z. Kuchinskii, N. A. Kuleeva, and M. V. Sadovskii, J. Exp. Theor. Phys. **120**, 1055 (2015); arXiv: 1411.1547.

22. R. Micnas, Acta Phys. Pol. A **100** (s), 177 (2001); arXiv: cond-mat/0211561v2.

23. M. Drechsler and W. Zwerger, Ann. Phys. (Leipzig) **1**, 15 (1992).

24. S. Stintzing and W. Zwerger, Phys. Rev. B **56**, 9004 (1997); arXiv: cond-mat/9703129v2.

25. M. V. Sadovskii, *Diagrammatics* (World Scientific, Singapore, 2006).

26. R. Bulla, T. A. Costi, and T. Pruschke, Rev. Mod. Phys. **60**, 395 (2008).

27. M. V. Sadovskii, *Superconductivity and Localization* (World Scientific, Singapore, 2000).